On the Impact of Time-varying Underwater Acoustic Channels on the Performance of Routing Protocols

Beatrice Tomasi*, Giovanni Toso†, Paolo Casari†‡, Michele Zorzi†‡

*Applied Ocean Physics and Engineering Department, Woods Hole Oceanographic Institution — 266 Woods Hole Rd, 02543 Woods Hole, MA, USA

†Department of Information Engineering, University of Padova — via Gradenigo 6/B, 35131 Padova, Italy

‡Consorzio Ferrara Ricerche — via Saragat 1, 44122 Ferrara, Italy E-mail: {firstname.lastname}@dei.unipd.it

Abstract

The recent development of underwater acoustic modems has enabled multihop networking capabilities that can be used in important military and civilian applications. For this reason, routing protocols for underwater acoustic networks (UANs) have recently been proposed and evaluated. However, the interactions between channel dynamics and networking performance are not well understood. In this paper, we investigate and quantify the effect of the time-varying link quality on routing protocols in static UANs. In order to do so, we simulate the considered routing protocols in several network scenarios, obtained by changing the network density, the number of packet retransmissions, the packet length, the modulation type and the power level with both time-varying and time-invariant channel conditions. Results confirm that, when evaluating the performance of routing protocols, it is important to understand the time-varying behavior of the channel quality over intervals of time sufficiently long to accommodate multihop communications. Finally, we also present experimental results, confirming the outcome of the simulations. The experiments have been conducted in collaboration with the NATO Centre for Maritime Research and Experimentation (CMRE) during the Commsnet12 sea trial.

Index Terms

Underwater acoustic networks, time-varying channels, source routing, flooding, network performance evaluation.

I. INTRODUCTION

Networking capabilities in underwater acoustic communications enable several applications of both civilian and military interest, such as environmental monitoring and coastal surveillance. These applications often rely on network communications over multihop topologies. However, small available bandwidths as well as long propagation delays and high error rates represent challenges to the design of optimal communication and networking algorithms.

The goal of this paper is to make a step towards a better understanding of how channel conditions and their dynamics in time and space affect the performance and the design of communications protocols in an underwater acoustic network. To do so, we leverage on the availability of some data collected in some sea trials and investigate them through analysis and simulation, in order to gain some insight about how fundamental routing approaches are affected by channel behaviors. We do not focus on a detailed comparison of the considered schemes per se, which would require a bigger set of more advanced routing protocols to be studied, but rather try to characterize the behaviors of broader classes of schemes through representative examples.

Scientists have only recently studied and not yet fully characterized the time and spatial variability of link qualities in a multihop network scenario. In fact, modeling sound propagation in the water volume is still an open research area, and the models that accurately reproduce the sound pressure (e.g., see [1]) also require a sufficiently rich description of the environmental conditions over both time and space. Therefore, in order to effectively represent the physical UWA link in networking studies, we make use of the channel quality dynamics measured over intervals of time relevant for both point-to-point and network communications. Some examples of recent work on channel dynamics over time scales important for networking can be found in [2]–[7].

Starting from these results, we study how time-varying channel conditions affect the performance of representative routing protocols in shallow water static networks. In particular, the main aim of this work is to evaluate the impact of the time fluctuations observed at frequencies used for communications (from 10 to $25\,\mathrm{kHz}$) in multihop scenarios and for different routing paradigms. We focus on the interplay among three parameters: i) the acoustic propagation delay

among nodes in the network, ii) how stable the link quality is over time, and iii) the time required by the routing protocol to establish and maintain a path from the source to the destination, when this mechanism is employed.

To the best of our knowledge, similar contributions are missing in the literature. Several routing protocols have been recently proposed for UANs (e.g., see [8]–[12]), following different paradigms in terms of fundamental approach as well as routing metrics for path selection. Examples include geographic routing, source routing, energy-aware routing, etc. For the purposes of our study, the main differentiating factor among the various options is the amount of signaling overhead, i.e., the total cost incurred by the network to deliver a data packet. From this viewpoint, and to gain some basic understanding on how channel dynamics affect different routing paradigms at a fundamental level, we consider in this paper two somewhat extreme approaches, namely source routing (which uses signaling for both path establishment and path maintenance) and flooding (which uses essentially no overhead). Other routing approaches not explicitly considered here are likely to show behaviors that fall somewhere in between these two extremes, although any advanced routing protocol (e.g., geographic routing, which requires control messages to establish the area toward which the node propagates the packet) may be expected to have an overhead that is closer to that of source routing than to that of flooding. Note that reactive protocols may become inefficient in large scale networks as every source consumes energy and bandwidth resources in transmitting control packets to establish the path. For this reason, in large scale networks proactive routing may represent a better option. However, typical underwater acoustic networks are sparse, i.e., at most a few tens of nodes are deployed, as acoustic waves reach longer ranges than any other type of wave under water. This also means that large scale networks would lead to large multiuser interference in the underwater acoustic context. As the set of issues arising from a detailed study of large-scale scenarios and the resulting reliability analysis are beyond the scope of the present paper, we leave them as an interesting item for future work.

The protocols in the literature have been evaluated by means of simulations, where, however, channel realizations are often time-invariant. Such strong assumption makes the results less representative of the protocol performance in practical scenarios where channel dynamics play a key role. A further effort in evaluating networking protocols performance by means of more accurate channel representations can be found in [13], [14], where an acoustic ray tracer is

employed in order to compute channel power gain realizations. Even though these contributions are useful to evaluate the impact of spatial channel variability on the network performance, the channel quality is maintained constant throughout the simulation time, thus limiting the impact of the results.

Our approach differs from such previous works, since i) we reproduce the temporal channel quality fluctuations, measured during at sea experiments, over time scales of interest for networking multihop protocols; ii) we perform a simulation study on the impact of such time-varying channel qualities on the performance of two protocols, which are reasonable examples of routing strategies representing a complex case (source routing) and a basic case (flooding); iii) we consider different types of packet lengths, numbers of retransmissions, network densities, modulation schemes, and source levels; iv) we evaluate the results obtained from a real data set collected during the Commsnet12 at-sea experiment; and v) we look for fundamental relationships between channel dynamics and networking protocol performance and design.

The obtained results highlight the importance of reproducing the channel fluctuations occurring over time intervals of a few seconds or even minutes, when evaluating multihop networking protocols. Moreover, both simulation and experimental results suggest that path establishment procedures that may be long compared to the packet length result into inefficiencies in terms of both throughput and energy consumption.

II. Dynamics of the quality of underwater acoustic channels

In this section, we present and discuss the in band Signal to Noise Ratio (SNR) time series measured during different experiments. The main goal is to provide examples of the dynamics of the channel quality over intervals of time that can affect the performance of networking protocols. Motivated by these observations, we then evaluate how much the communication performance is affected by these dynamics.

The SNR is a function of the channel gain, the noise power spectral density and the transmitted power. The latter is constant during the considered experiments, and therefore the observed dynamics only depend on the time variability of the noise level and of the channel gain. However, the noise level changes over long intervals of time (hours), whereas the channel gain can actually change over short intervals of time (seconds) [15]–[17]. Therefore, the measured SNR dynamics are a sufficient representation of the time-varying channel gain that occurs in underwater acoustic

communications.

In the literature, the channel is typically modeled as a filter consisting of a finite number of coefficients, which are complex gain values (α_i), and delays (τ_i). The channel impulse response can be expressed as:

$$c(t) = \sum_{i=0}^{L} \alpha_i \delta(t - \tau_i). \quad (1)$$

If both α_i and τ_i do not depend on t, then the channel impulse response is time-invariant. In the following, we consider this case when the ray tracer is fed with constant environmental parameters. If either coefficients or delays (or both) depend on t ($\alpha_i(t)$ and/or $\tau_i(t)$), then the channel impulse response is considered time-varying. In our simulations, we will also consider this case by using time-varying sound speed profiles as an input to the ray tracer.

A. Time-varying channel quality observed during experiments

In this section, we present the SNR time series, as a representation of the acoustic channel fluctuations over intervals of several minutes. The importance of presenting these measurements (which can be considered as raw data) lies in: i) the fact that the observed channel fluctuations occur over time intervals affecting networking protocols; ii) providing a general representation of the channel dynamics, since they drive the evolution of the communication systems over time, without making any assumption on the physical layer used; iii) the lack of a model that represents such dynamics, which makes such raw data important to better interpret the obtained results. The resulting performance also depends on the parameters of the communication system, since a more robust scheme is less sensitive to SNR fluctuations. For this reason, here we chose to focus on the temporal properties of the physical link, instead of deriving communication metrics for a specific system.

In order to measure such temporal properties, several research groups have recently conducted experiments that consisted in transmitting and recording acoustic signals in shallow water. Such experiments are characterized by different durations, timing and locations. The collected data sets can therefore be used to evaluate the performance of different communication systems in a variety of coastal scenarios. The analysis of this data has highlighted that the quality of a static link exhibits dynamics over a time scale that is important for networking protocols, and that such fluctuations are environment-dependent. However, the identification and quantification

of the environmental conditions that cause such time-varying behavior are currently topics of ongoing research [2]–[4], [6], [7].

As an example of this recent activity, we present here some SNR time series, collected during three experiments: Surface Processes and Acoustic Communications Experiment (SPACE08), Submarine Network (SubNet09), and Kauai Acomms MURI (KAM11), which took place off the coast of Martha's Vineyard (MA-USA), Pianosa (Italy), and Kauai (HI, USA) islands, respectively. SPACE08 lasted from October 18 to 27 in 2008, SubNet09 started at the end of May 2009 and ended at the beginning of September 2009, and KAM11 was conducted from June 25 to July 9 in 2011. These experiments and the collected data are also described in [15]–[17]. These experiments lasted several days, thus making it possible to evaluate long-term channel quality fluctuations of stationary links. It is worth noticing that in these experiments the SNR is estimated differently, according to the communication system considered. In fact, during both SPACE08 and KAM11, the transmitted signals were sent using a coherent modulation scheme: for these data sets, we compute the average (over 1 s) SNR at the output of an equalizer, whose parameters are reported in [18] and [19]. Instead, during SubNet09, we employed several chirp pulses, from which we estimate the instantaneous values of the SNR, as measured by a non-coherent receiver. Since the SNR estimation methods and the SNR dynamics are quite different we show an example of SNR time series during SPACE08 and KAM11 in Fig. 1 and a time series for Subnet09 in Fig.2.

Fig. 1 shows the time series of the output SNR over three minutes during SPACE08 and KAM11. Note that the SNR during SPACE08 has more limited dynamics than that observed during KAM11. An explanation of this lies in the different propagation conditions. In fact, in SPACE08 transmitters and receivers are deployed in a very shallow water area (the water depth is approximately 15 m), and therefore this data reveals surface-dependent dynamics. Instead, during KAM11, the water column is approximately 100 m deep, thus making this data more informative on the dynamics caused by both surface and sound speed profile fluctuations over time.

Since the SubNet09 data contains SNR values measured once every 30 seconds, Fig. 2 shows a longer (two hours) time series. The channel quality exhibits large fluctuations throughout the observed interval (note that here the SNR is in the region $[5, 30]$ dB), and similarly to KAM11 (the water depth for SubNet09 is 80 m), the sound speed profile plays an important role in the

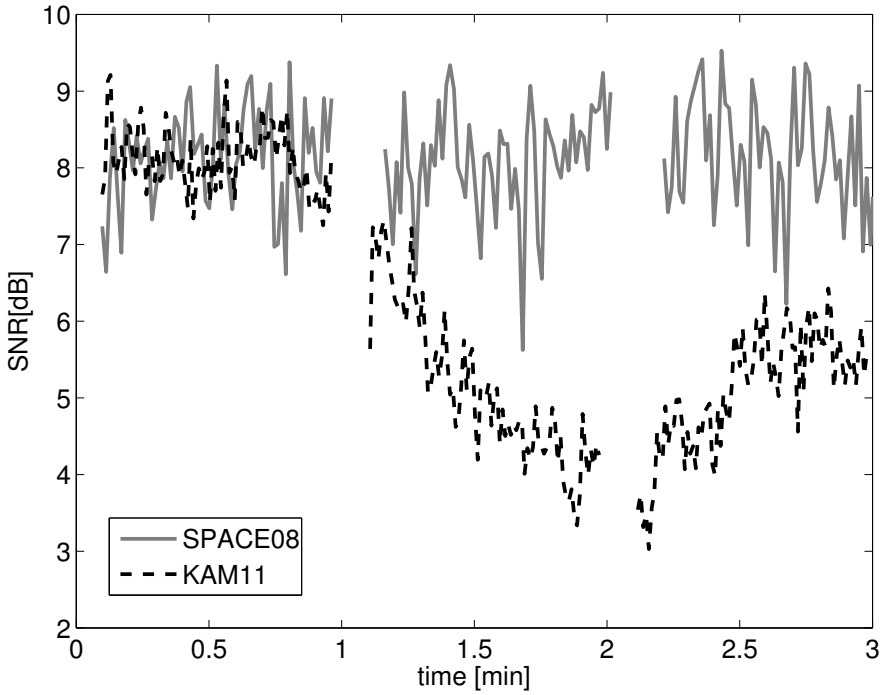

Fig. 1. Time series of the average SNR obtained at the output of an equalizer during SPACE08 and KAM11, represented with a solid gray and a dashed black line, respectively. In SPACE08, the transmitter and receiver were 200 m apart and the time series shown was recorded on October 19, 2008. In KAM11, the distance between the transmitter and the receiver was 3000 m and the measurements shown were taken on July 8, 2011.

dynamics of the channel quality, as analyzed in [20, p. 227–250].

In this paper, we will evaluate the performance of source routing and flooding, when such channel dynamics are considered. However, from a modeling point of view, reproducing these fluctuations for different scenarios and node placements is not a trivial task. In fact, since experimental SNR traces are available only for specific locations, they cannot be directly employed in networking simulations, where node placements are typically drawn at random. Therefore, we compute the channel gain using a ray tracer fed with measured time-varying environmental conditions: although this is a simplified approach, it is deemed to be sufficiently accurate for the purpose of this paper. A validation of this approach through at-sea experiments is presented in Section VI.

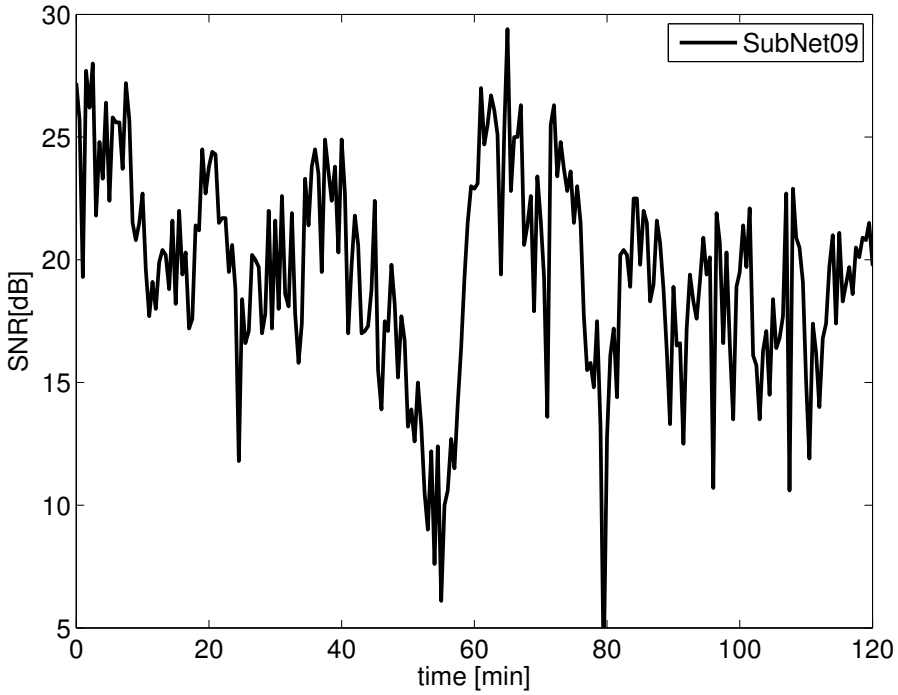

Fig. 2. Time series of instantaneous SNR in dB, measured during SubNet09, on May 31, 2009, between receiver 2, which was $40\ \mathrm{m}$ below the surface, and transmitter 1, $1500\ \mathrm{m}$ from the receiver.

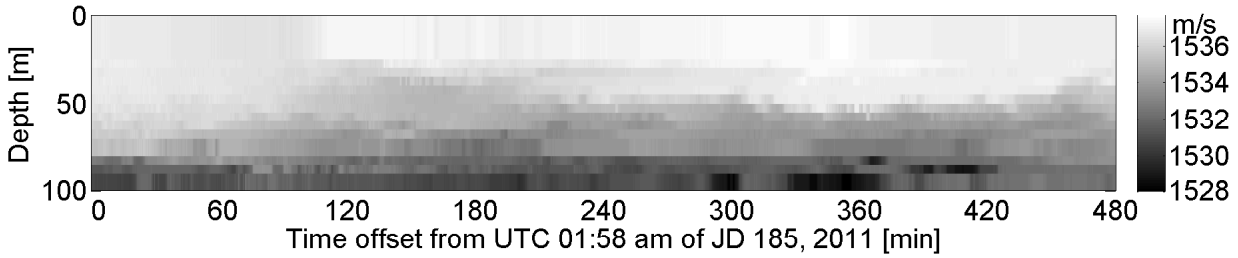

Fig. 3. Time series of the SSP measured once every 5 s for 8 hours during July 5, 2011. Darker shades of grey correspond to a lower sound speed. These values of the SSP are typical of a downward-refractive environment.

B. Time-varying channel quality computed through ray-tracing

The channel variability perceived by a non-coherent receiver can be well approximated using Bellhop [1]. To do this, we employ the set of sound speed profiles (SSPs) measured during

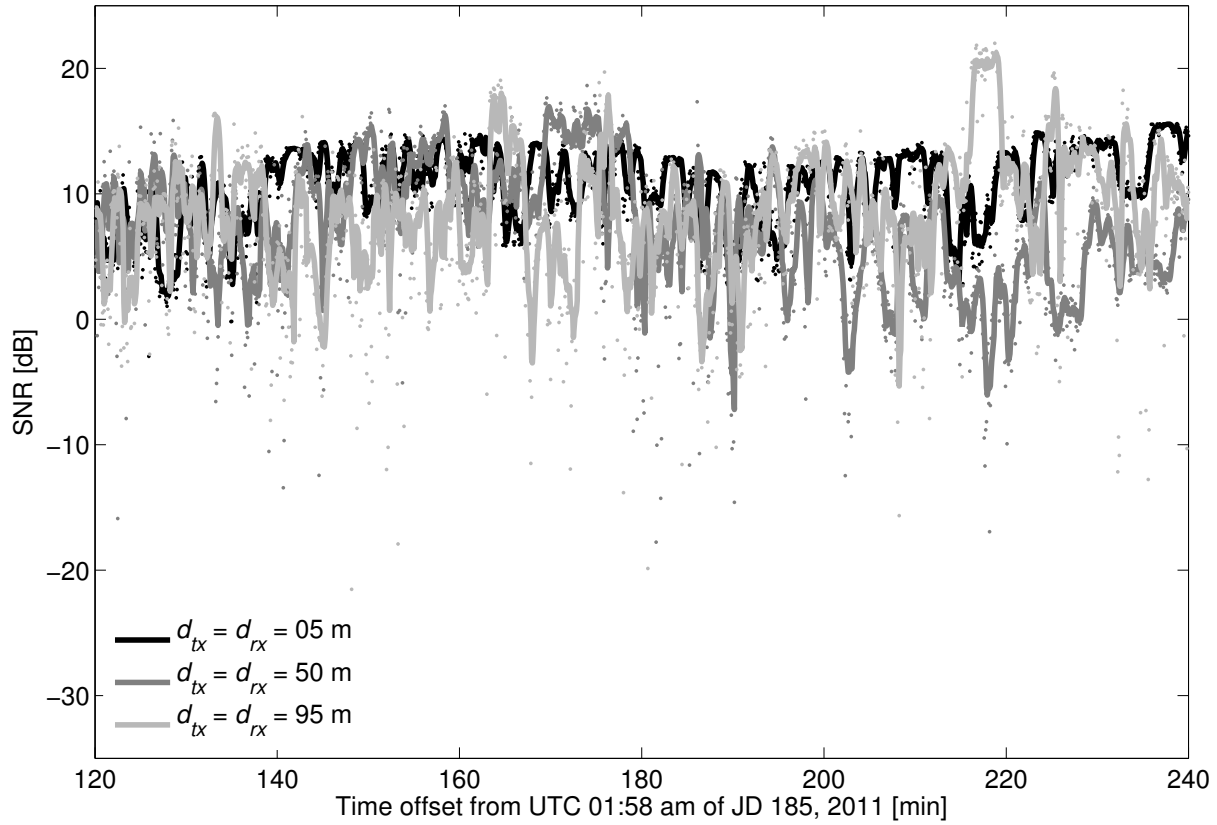

Fig. 4. SNR in dB as a function of time, $R = 1500$ m. The transmitter and the receiver are placed at the same depth; the traces show very similar behaviors. For each data set, the values of the SNR are shown as dots of the respective grey shade; a moving average taken over 6 samples (30 s) highlights the trend of the curves.

KAM11, where the water column was $100\ \mathrm{m}$ deep, and use it as an input to Bellhop. In order to model the other relevant environmental parameters, we consider a flat surface and bottom, and geoacustic parameters typical of rocky-muddy sediments. We focus on an interval of 8 hours in the KAM11 dataset, which includes one SSP sample every 5 s. For each sample, we compute the complex amplitude-delay profile of the acoustic channel as a function of the depth of the transmitter and of the receiver, as well as their range.[1] The amplitude-delay profile is post-processed, for each transmitter depth d_{tx}, receiver depth d_{rx} and transmitter-receiver range R, by summing the complex amplitudes of all arrivals, and by taking the square of the magnitude of the

[1]Similar to the Bellhop jargon and akin to [21, Ch. 3], the range is defined as the planar distance between the nodes, i.e., as the distance projected on a plane parallel to the sea floor.

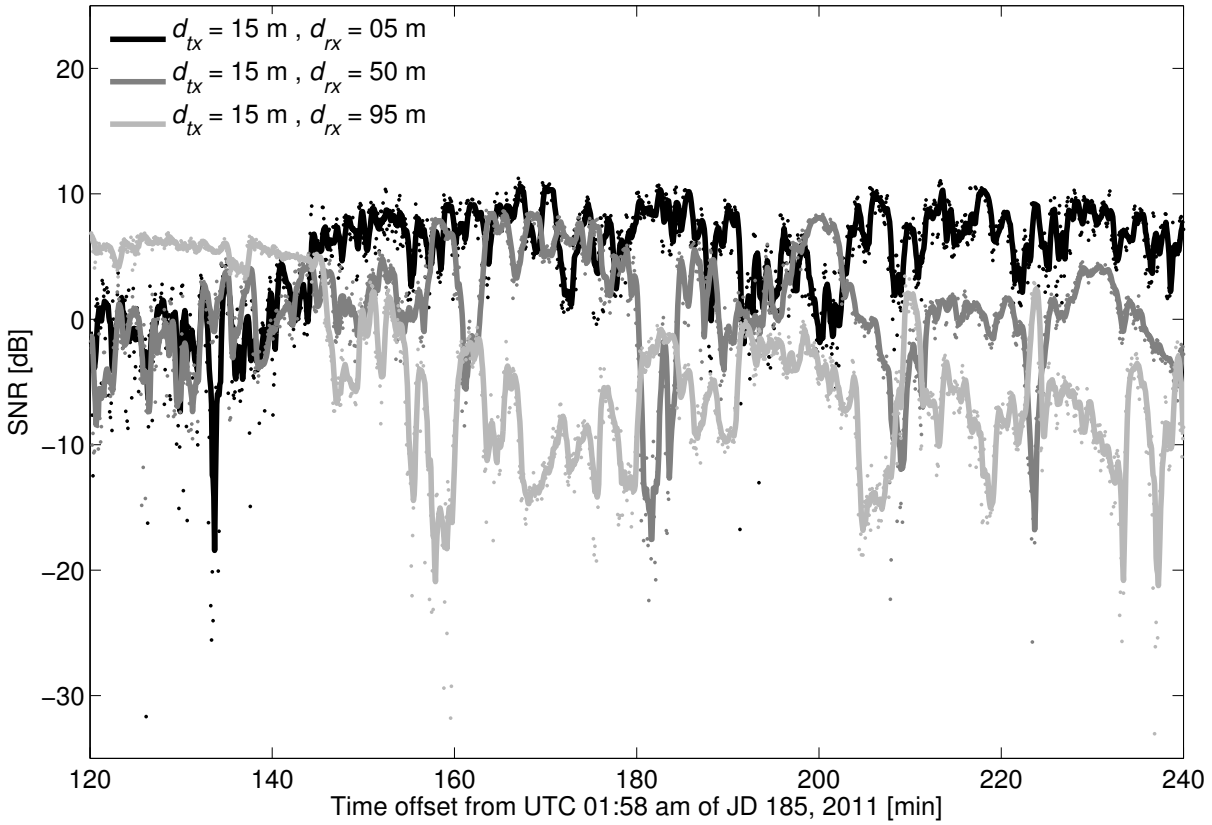

Fig. 5. SNR in dB as a function of time, $R = 3000$ m, $d_{\rm tx} = 15$ m, whereas $d_{\rm rx}$ is 5, 50 or 95 m. For each data set, the instantaneous values of the SNR are shown as dots along with their 6-sample moving averages, as in Fig. 4. All traces show periods of stability with minor local oscillations, as well as occasionally deeper fades.

resulting sum in order to yield the channel power gain ($|\sum_{i=0}^{L} \alpha_i|^2$). With this information, and knowing the transmitted power, the transmit frequency and the system bandwidth, the SNR can be derived. Since the SSP changes over time (see Fig. 3), the channel power gain also changes. Fig. 4 exemplifies the fluctuations of the SNR over three underwater links, where the transmitter and the receiver are deployed at the same depth ($d_{\rm tx} = d_{\rm rx} = 5$, 50, or 95 m) and at a range $R = 1500$ m. A window of 2 hours (out of the 8 hours depicted in Fig. 3) is considered. The three SNR curves show a very similar behavior, whereby the average SNR is stable in the long term, but local oscillations of 10 to 20 dB (peak-to-peak) are observed over intervals of around 3 minutes. Some deep fading events where the SNR decreases below 0 dB are also experienced by the links at 50 m and 95 m of depth. Fig. 5 shows a slightly different setup, where the

transmitter is placed at $d_{\rm tx} = 15$ m and the receiver is at a range of $R = 3000$ m and at a depth $d_{\rm rx} = 5$, 50, or 95 m. The long-term difference between the values of the SNR over the three links is more remarkable in this case, although local variations of similar size, as in Fig. 4, also occur.

Therefore, by feeding Bellhop with time-varying propagation conditions, we are able to reproduce channel quality fluctuations similar to those measured at sea. This makes it possible to derive the statistics of the networking performance for different protocols and scenarios, as presented in Section V.

III. Description of the example protocols

Following the classification presented in [22], we consider among the many possible routing protocols two representative solutions characterized by very different amounts of overhead, namely one based on source routing and a second one based on flooding. We consider a single source scenario, thus leading to an optimistic performance evaluation (since multiple source scenarios would lead to a higher interference). However, we point out that this study focuses on the effect of UWA channel dynamics on routing protocols that require different amounts of signaling overhead, rather than on a direct protocol comparison. For the reader's convenience, in this section we summarize the basic operations of the two protocols. More details can be found in [23].

A. Source routing for Underwater Networks (SUN)

SUN separately defines the behavior of sinks and nodes, which are treated as two different entities in the network. Sinks are only responsible for periodically broadcasting probe messages, that notify their presence to their neighbors, and for receiving data packets. All other nodes can send data, ask for paths, answer path requests, act as relays, and notify broken routes. Among these nodes we distinguish those, called "end nodes", that receive probes sent by the sink, and are therefore directly connected to it. When a node has data to transmit[2] and its hop count to the sink is greater than 1, it sends the data to the next hop, if known, otherwise it initiates a path discovery process.

[2]This node will be called source.

The path discovery process is similar to that of Dynamic Source Routing (DSR) [24]: a source node broadcasts a path request, which is flooded through the network until an end node is reached. In order to avoid loops in the path, every relay node that receives a path request checks whether or not its address is already in the header of the packet. If not, it writes its network address in the header and rebroadcasts the path request. When the path request reaches an end node, it creates a path reply packet, and sends it back in unicast following the sequence of addresses (in reverse order) written in the header of the path request. If multiple paths reaching the sink exist, the source may receive multiple path replies, among which it chooses the best route according to a predefined metric. In this paper, the metric is the SNR, and more specifically, the path with the largest (among all the paths) minimum SNR (among the links of a route from source to destination) is chosen. This policy has been shown to yield good throughput results in [18]. Ties are broken by picking the route in the earliest path reply received by the source. The chosen route is stored and has an expiration time. If the source still has traffic to send to the sink and if the valid route has expired, a new path discovery is initiated.

After a path is established, data is sent to the chosen next hop by the source. In general a packet, either generated or to be relayed, is queued in a buffer at each node. The buffer is periodically checked and the queued packets, if any, are served according to a First-In-First-Out (FIFO) policy. When data is correctly received by the next hop, an ACK is sent to the transmitter, and the forwarding process continues. Otherwise, after the ACK timeout expires, up to F retransmissions are allowed. In fact, SUN has full control over link layer retransmissions so that control packets are not retransmitted, and a packet failure can trigger a new path discovery process only after F retransmissions. This translates into higher reliability and shorter latency than having to initiate a new path discovery process every time a data packet is lost. If these retransmissions fail as well, the transmitting node notifies upstream a link failure through a path error packet, which triggers a new route discovery process.

In this paper, we analyze SUN under different working regimes defined by: i) a low constant data rate traffic, representative of an application that does periodic monitoring; ii) varying network densities; iii) a static topology; iv) F retransmissions of data packets; v) packet length P; and vi) time-varying and time-invariant channel conditions. Moreover, we consider a network with only one source and one sink. Such case study aims to better understand how geometry, distances, channel conditions, and packet length affect the performance of source routing under

time-invariant and time-varying channels.

B. Flooding in underwater acoustic networks

A flooding-based routing protocol is the simplest solution to route a packet from a source to a sink, since it only requires a decode and forward operation at each relay until the packet reaches the sink. In this paper, the considered protocol also avoids loops in the forwarding process, i.e., if the node has already received a data packet, which is uniquely identified by its sequence number, then it does not forward it. Moreover, the flooding protocol includes neither an acknowledgment mechanism for correctly received packets, nor the retransmission of lost packets. Therefore, flooding is characterized by the absence of feedback, of control packets, and of a mechanism to select a best path, and can be thought of as a best effort solution.

In terrestrial radio networks, flooding-based routing gives rise to inefficiencies in terms of both network capacity and energy consumption, since the more the nodes, the higher the multi-user interference, thus leading to a performance degradation and to an increased energy consumption. Therefore, this protocol is often used together with other optimization mechanisms, or forwarding policies, in order to mitigate the interference and energy consumption problems.

In this paper, we analyze flooding under the same conditions considered in SUN, except for the use of retransmissions. This case study focuses on the impact of network deployment and channel quality on the protocol performance.

IV. Simulation scenario

SUN and flooding have been implemented in the NS-Miracle simulator [25]. The employed channel models are: i) a time-invariant channel attenuation model based on empirical equations for acoustic power spreading and absorption, presented in [26, p. 99–202], and in [27], and ii) a time-varying channel gain as derived in the study of Section II-B. In the latter case, we assume that the computed time series of the power gains is a sufficient description of the channel dynamics, and that it depends only on the transmitter and receiver depths and their range. This means that the angle between the transmitter and the receiver in the horizontal plane does not affect the channel power gain, since also the sea floor and the surface are considered flat throughout the area. The physical layer is modeled as a Binary Phase Shift Keying (BPSK) modulation scheme with a bandwidth of 4 kHz and a bit rate of 2048 bps. The center frequency

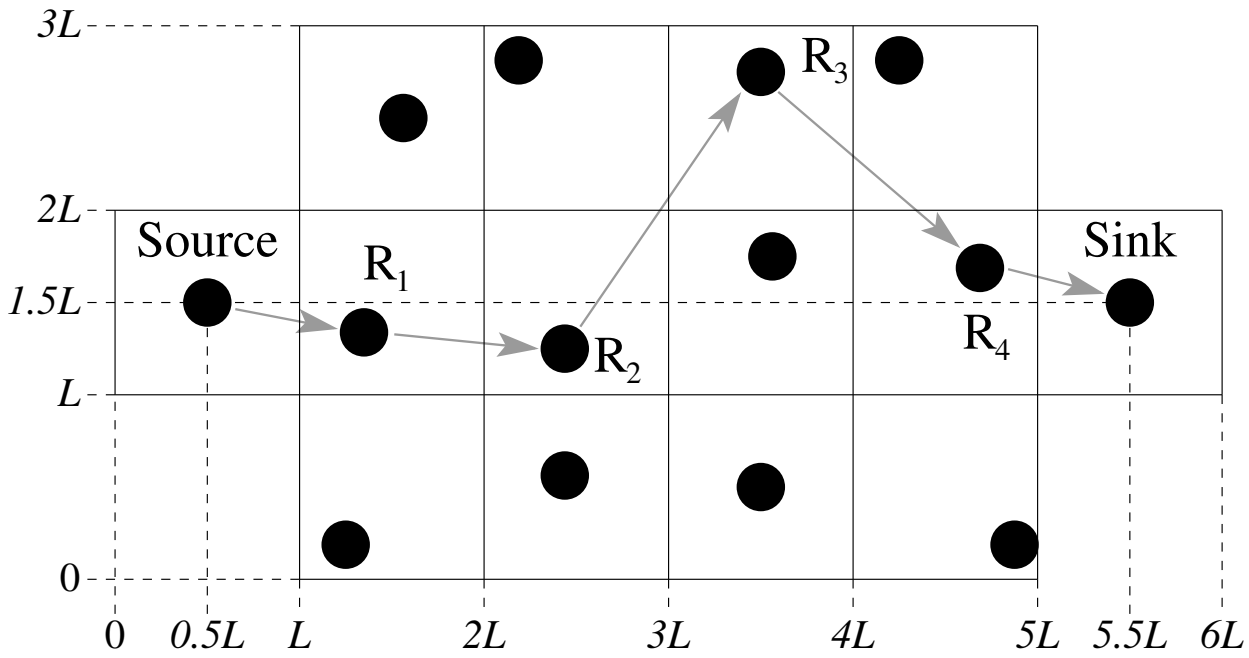

Fig. 6. Schematic representation of the simulation scenario as seen from above. Only the source on the left generates packets, which are routed to the sink on the right through the relays in between. The area in the middle is subdivided into 12 cells of volume $L \times L \times 95$ m^3. All nodes are deployed at the same depth of 45 m.

is 25 kHz and the transmit power is set to 150 dB re μPa. By employing the channel gain as in i) and ii), and by obtaining the noise power through the empirical equations in [26], [27], we compute the Signal-to-Noise Ratio (SNR). Moreover, the power of any interfering signal is also treated as additive noise, and the SNR is adjusted accordingly. We then evaluate the packet error probability by using the BPSK bit error rate equation, i.e., $BER = Q(\sqrt{2\gamma})$, which is expressed as a function of the SNR, γ, and by assuming independent bit errors and no coding.

In the simulations of both SUN and flooding, the considered Medium Access Control (MAC) protocol is based on Carrier Sense Multiple Access (CSMA). This means that when a node has a packet to transmit (either generated or to be forwarded), it first senses the channel, and the transmission starts only if the channel is clear. Otherwise, if the channel is sensed busy, the packet is backlogged and further channel sensing phases are performed in a 1-persistent fashion, until the channel is sensed idle and the transmission can take place.

The considered deployment is shown in Fig. 6, where the network area is observed from above. Among the 14 nodes, the leftmost is the source and the rightmost is the sink. The water

in the deployment area is assumed to be 95 m-deep, and the whole water volume is divided into cells of $L \times L \times 95 \ \mathrm{m}^3$, where L is the length of the side of each cell. The source and the sink are centered within their respective cells, whereas each of the 12 relays is placed uniformly at random in one of the remaining 12 cells. All nodes are deployed at a depth of 45 m. In the simulations, we vary the cell side L from $500 \ \mathrm{m}$ to $2500 \ \mathrm{m}$ with a 100 m step, so as to evaluate the protocol performance over different network densities. We increase the cell side length, since the only channel dynamics affecting the protocol performance are those triggering unsuccessful receptions, e.g., when the average SNR is sufficiently low.

Data traffic is exclusively and periodically generated by the source at a rate of one packet every two minutes. We consider two packet sizes: $P_1 = 8 \ \mathrm{kbit}$, and $P_2 = 1 \ \mathrm{kbit}$, corresponding to packet durations of 4 s and 0.5 s, respectively. Moreover, in the simulations of SUN, we consider two values for the maximum number of allowed data packet retransmissions[3], $F_0 = 0$ and $F_4 = 4$. The following section is devoted to presenting the results obtained in the scenarios here described, and to discussing their implications on networking performance and design.

V. Performance results

The performance of SUN and flooding is evaluated in terms of throughput, end-to-end delay, and network transmit energy consumption. Throughput is defined as the amount of data traffic that is correctly delivered to the sink per unit time, and is measured in packets per minute. The end-to-end delay is the amount of time between the packet transmission and its successful reception and is expressed in seconds. The network transmit energy consumption is the total amount of energy consumed by the whole network for transmission[4] and is measured in Joule. We here analyze these three metrics, since they provide a comprehensive representation of key aspects in typical applications for UANs. For example, throughput is an important metric in monitoring applications, which require the maintenance of a minimum data rate. Instead, end-to-end delay becomes a key metric in alert systems for surveillance applications, and network

[3]For the sake of clarity, one retransmission means that the same data packet has been transmitted by the same node twice.

[4]We consider a transmit power consumption of 3.3 W, akin to that of the cNode transponder by Kongsberg Maritime [28]. Moreover, for simplicity we do not consider energy consumed for reception and idling, as it similarly affects both protocols and is negligible with respect to the amount of energy consumed for transmission in an underwater acoustic modem.

transmit energy consumption is particularly important when nodes are battery-powered, since their lifetime also depends on the amount of energy consumed for communications.

Therefore, the average value of these metrics is evaluated by means of simulation for different cell side lengths L in the deployment shown in Fig. 6. In particular, we focus on:

- the performance of SUN and flooding under time-varying vs time-invariant channel realizations;
- how the performance of SUN improves or decreases, and what are the trade-offs involved when retransmissions are employed;
- the performance evaluation with long and short data packets.

This section is organized as follows: we first analyze the performance of reactive routing (in this case, SUN) and flooding separately with both time-varying and time-invariant channel conditions, then we compare their performance, by highlighting the interplay among the channel coherence time, the network density, and the communication system parameters, and finally we consider the impact of different constellation sizes and source levels on the study performed.

A. Performance of reactive routing

Figs. 7, 8, and 9 show average throughput, end-to-end delay, and network transmit energy consumption as a function of L, respectively. When results are obtained by using time-invariant (time-varying) channel realizations, the curve is labeled as TI (TV) and indicated with a circle (triangle). The label P_1 (P_2) represents the case of packet size equal to 8 kbit (1 kbit), whereas F_0 (F_4) means that 0 (4) retransmissions are allowed.

In Figs. 7, 8, and 9 we can distinguish three regions:

- $L < 900$ m, where single-hop routes are chosen;
- $900 \leq L < 1900$ m, where two-hop routes are chosen;
- $L \geq 1900$ m, where three-hop routes are chosen.

In the first region, the source receives from the sink the probe messages, sent periodically every 30 seconds. Such probes are sensed with an SNR greater than a threshold (here set to 10 dB), and therefore the source can directly forward the data to the sink. This means that path discoveries do not start and interference-free communications occur. This translates into a linearly increasing end-to-end delay with L, as shown in Fig. 8, and also implies that the packet

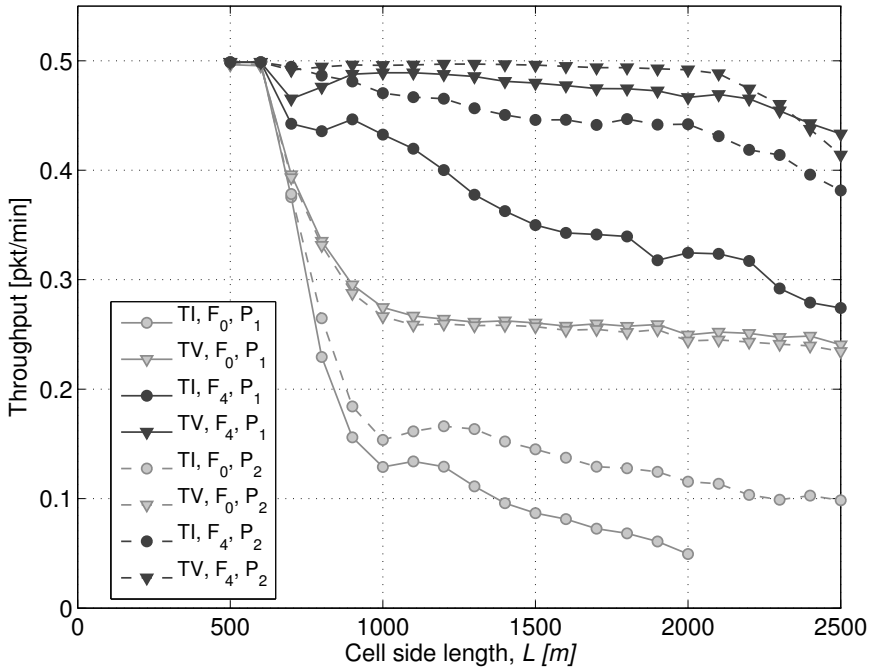

Fig. 7. Average throughput as a function of the cell side length L for SUN. Results obtained by using time-invariant (time-varying) channel realizations are labeled as TI (TV) and indicated with a circle (triangle). The label P_1 (P_2 and dashed line) indicates packet size equal to 8 kbit (1 kbit), and F_0 (F_4 with black curves) corresponds to 0 (4) retransmissions.

error rate, PER, only depends on the channel attenuation, which in turn is a function of the single-hop distance, which in this case is proportional to the cell side length, L.

In the second and third regions, the throughput decreases more slowly, since multi-hop routes are established. Note that time-varying channel conditions become beneficial to the throughput. This is caused by: i) the chosen metric for route selection, which is the maximum minimum SNR in the path, and ii) time diversity of the channel conditions. The considered metric implies that the bottleneck link in the selected route is the shortest among the longest hops in all possible routes. Moreover, as will be explained in the following, shorter hops also present more stable dynamics, and are therefore less likely to cause path failures. For this reason, also the end-to-end delay is smaller for the TV than for the TI channel conditions, as shown in Fig. 8. In fact, in TI channel conditions, the bottleneck link is the same throughout the simulations, whereas that selected in TV channels changes with the channel quality, thus resulting in a shorter (on average) link, and propagation delay. The energy increases at $L = 900$ for both TV and TI cases with

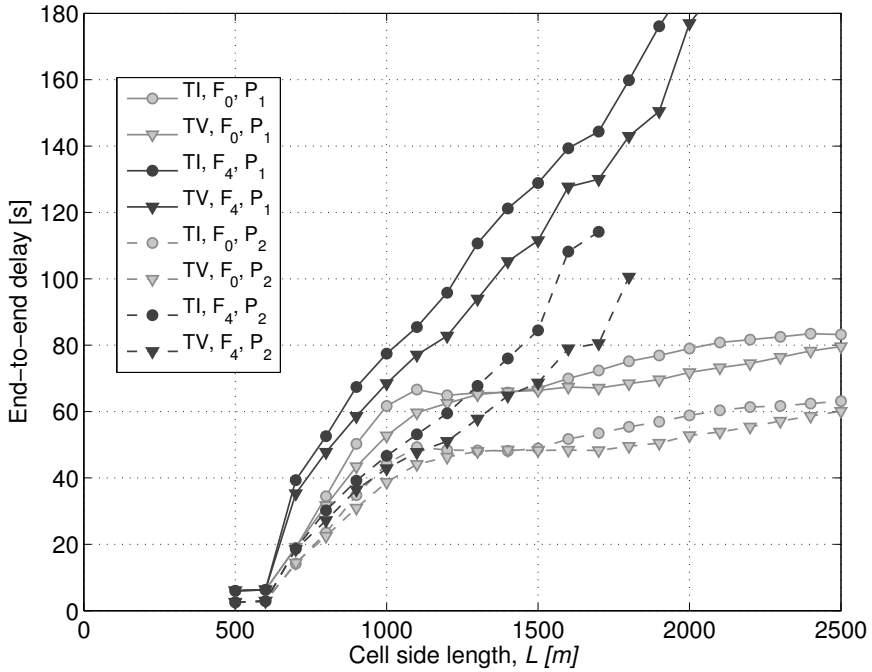

Fig. 8. Average end-to-end delivery delay as a function of the cell side length L for SUN. Results obtained by using time-invariant (time-varying) channel realizations are labeled as TI (TV) and indicated with a circle (triangle). The label P_1 (P_2 and dashed line) indicates packet size equal to 8 kbit (1 kbit), and F_0 (F_4 with black curves) corresponds to 0 (4) retransmissions.

packet length P_1, since even though two-hop paths start occurring in the simulations, sometimes also single hops are still chosen. In these latter cases, four retransmissions are allowed per unsuccessful reception, which is more likely due to the long single hop distance, and therefore the increase of energy consumption is much greater than when no retransmissions are allowed.

In order to clarify the aforementioned relationship between the hop distance and the channel coherence time, we discuss a simple model in the following. Consider a linear topology, with N nodes deployed equally spaced at a distance R from each other, and where each node is forced to transmit the data to the next in the line. Assume that the durations of control packets (acknowledgments and path requests/replies) are negligible with respect to the duration of the data packets and the propagation delays. We define the *reactiveness* of the protocol, ρ, as the inverse of the maximum end-to-end delivery delay. Such end-to-end delivery delay, which includes both path discovery and data packet delivery, can be expressed as

$$T = \frac{(N-2)RTT}{M} + (N-1)(t_{\mathrm{data}} + RTT) \tag{2}$$

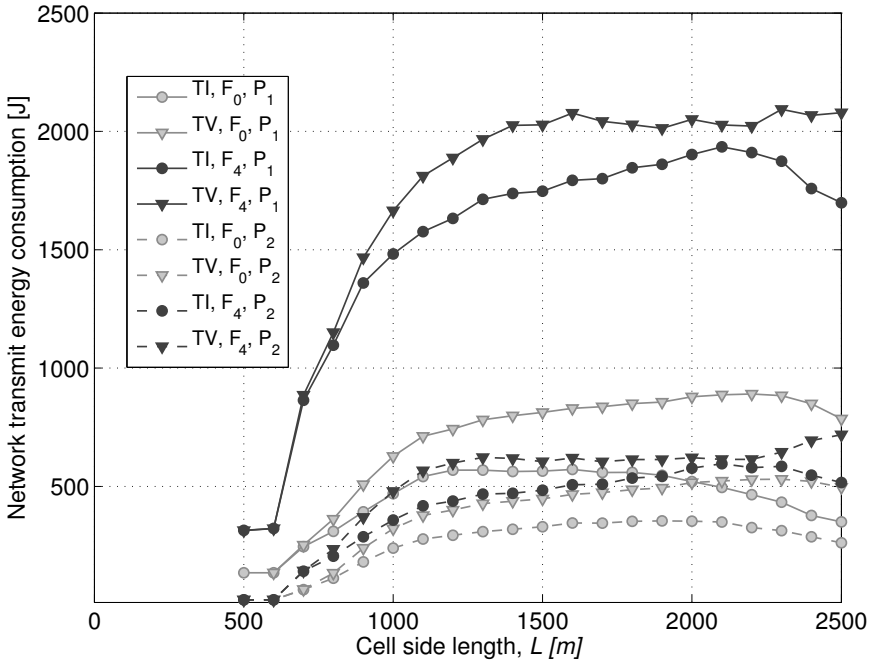

Fig. 9. Average transmit energy consumption in the network as a function of the cell side length L for SUN. Results obtained by using time-invariant (time-varying) channel realizations are labeled as TI (TV) and indicated with a circle (triangle). The label P_1 (P_2 and dashed line) indicates packet size equal to 8 kbit (1 kbit), and F_0 (F_4 with black curves) corresponds to 0 (4) retransmissions.

where M is the number of packets that can be delivered between two phases of path establishments, RTT is the one-hop round-trip time and $t_{\rm data}$ is the duration of the data packet transmission. The round-trip time includes the propagation delays in both packet transmission and ACK reception, and depends on the distance, R, between two neighboring nodes, as $RTT = 2R/c$, where c is the sound speed. In this way, the reactiveness of SUN is expressed as a function of the single hop distance, R, and the length of a data packet, $t_{\rm data}$. In order to obtain a stable reliable path, ρ should be larger than the variability rate of the communication performance.

Fig. 10 shows ρ as a function of the single-hop distance between two subsequent nodes in the line, R, for a 1 hop scenario, i.e., $N = 2$, and for two and three hops ($N = 3$ and $N = 4$, respectively). We consider $t_{\rm data} = 4$ s, and M is obtained by considering that each path expires every 12 minutes. Note that the x-axis represents the single hop distance over which the packet is forwarded, whereas in Fig. 7, L indicates the cell side of the deployment area for simulations. Fig. 10 shows that when multiple hops are chosen, i.e., N increases, source routing becomes more

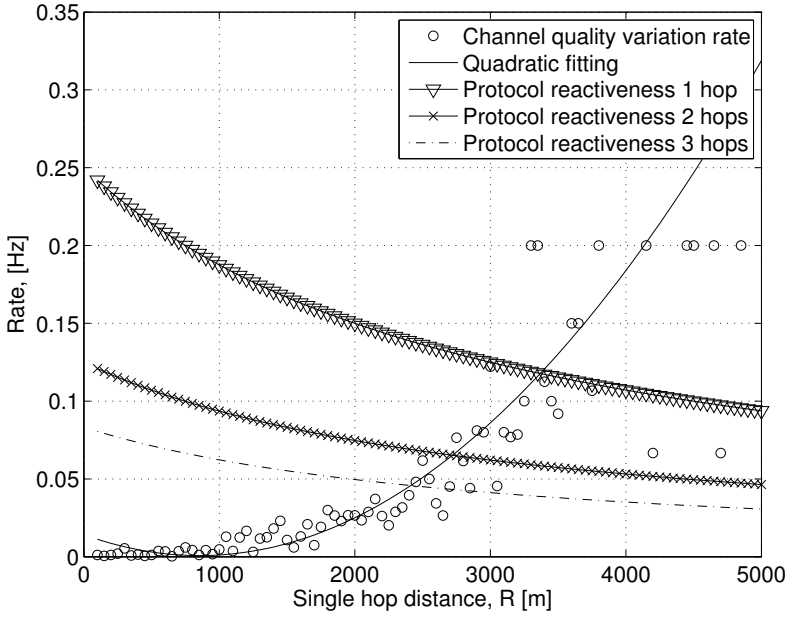

Fig. 10. Relationship between the protocol reactiveness as a function of single hop distance compared with the variability rate of the communications performance in circles, here indicated as channel quality rate.

sensitive to the channel fluctuations (the reactiveness curve shifts towards the left). However, as the hop distance becomes shorter, the channel variation rate decreases. Circles represent the inverse of the estimated coherence time of a reliable link, named channel quality variation rate here. This estimate is obtained by using the traces computed in Sec. II-B. A link is reliable when it belongs to a given region (here above 18 dB, where the BER is approximately 0). As shown in Fig. 10, the rate of the channel quality becomes greater than the reactiveness of the protocol in the single-hop scenario when the nodes are more than 3500 m apart, which is approximately the distance between the source and the destination at which the protocol starts choosing two-hop paths (i.e., when $L > 900$ m).

We now briefly discuss the impact of the packet length on the obtained results. The longer a packet, the higher the error probability, thus resulting in lower throughput, longer latency and larger energy consumption for P_1 than for P_2. Note that the throughput shown is measured in packets per minute in order to represent both plots in the same figure. Therefore, in terms of correctly delivered bits per minute P_1 has higher throughput. This indicates that the increased

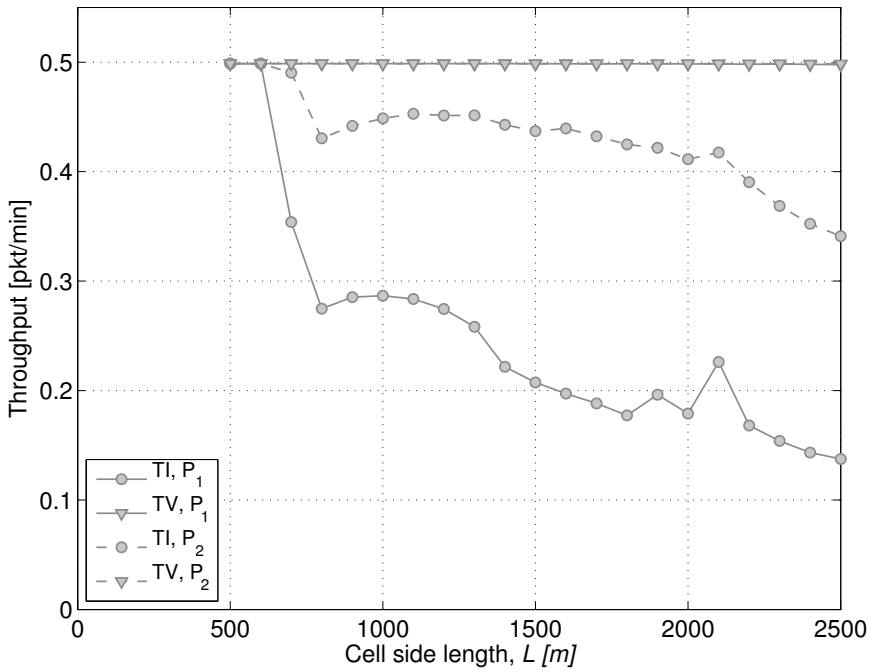

Fig. 11. Average throughput as a function of the cell side length L for flooding. Label P_1 (P_2 in dashed lines) indicates packet size 8 kbit (1 kbit), and the results obtained with time-varying (time-invariant) channels are labeled as TV (TI) and represented with triangles (circles).

of packet error for P_2 is compensated by the increased efficiency due to the higher number of bits transmitted in a round trip time.

Curves F_0 and F_4 differ for the number of retransmissions. The throughput for case F_4 is higher than that for case F_0 since the traffic rate is very low, and therefore after a packet is generated there is enough time to retransmit the information in case it is lost, without penalizing the next packet arrivals. This also translates into higher end-to-end delay and energy consumption for F_4 than for F_0.

B. Flooding performance

The average throughput, end-to-end delay, and network energy consumption of flooding are shown in Figs. 11, 12, and 13, respectively. We show the results for packet sizes P_1 and P_2, and for time-varying (TV) and time-invariant (TI) channel conditions.

In Fig. 11, we can again distinguish three regions

- $L < 900$ m, where mostly single-hop routes between the source and the destination occur;

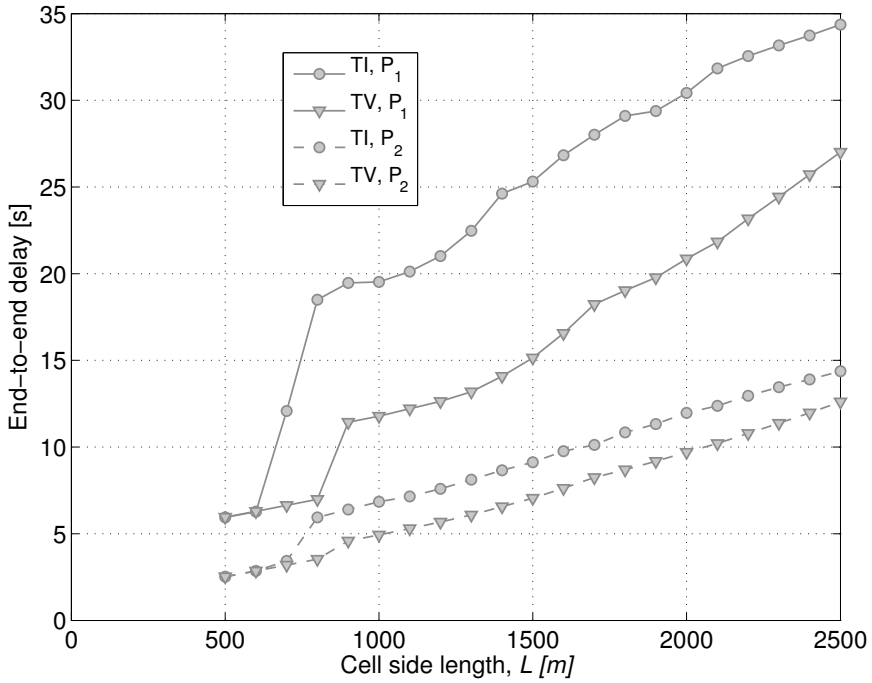

Fig. 12. Average end-to-end delivery delay as a function of the cell side length L for flooding. Label P_1 (P_2 in dashed lines) indicates packet size 8 kbit (1 kbit), and the results obtained with time-varying (time-invariant) channels are labeled as TV (TI) and represented with triangles (circles).

- $900\,\mathrm{m} \leq L < 2000$ m, where mostly two hop routes are used to reach the destination;
- $L \geq 1900$ m, where mostly three hop routes are used to reach the destination.

In Fig. 11, we show that for packet length P_1, the throughput (in packets/min) in TV channel conditions is higher than in TI channels, since the channel diversity generated by time-varying conditions decreases the interference among relays. The same gap in performance is not visible in the plot for packet length P_2, since in this case both scenarios have high throughput. This is due to the fact that shorter packets are more reliable than long ones and are less likely to cause multiple-access interference. Note that for TI curves as soon as the number of hops increases, the throughput improves, since on average the bottleneck link becomes more reliable. This is represented in Fig. 11 around $L = 900$ and $L = 2100$.

Fig. 12 demonstrates how the end-to-end delay increases as the network becomes sparser. Such delay increase does not translate to a decrease in throughput since the time interval between successive packets (30 seconds in this case) is larger than the delivery delay.

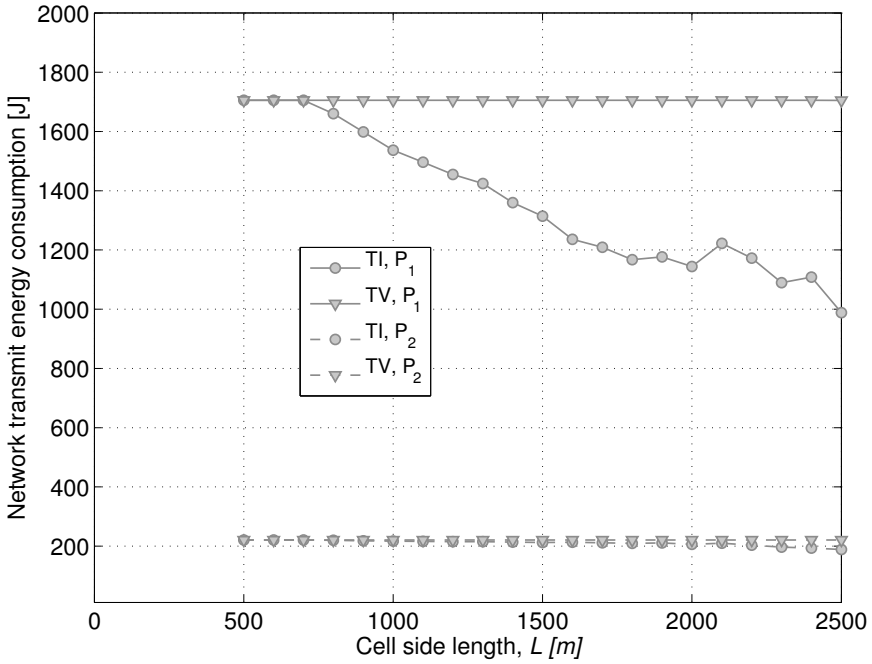

Fig. 13. Average transmit energy consumption in the network as a function of the cell side length L for flooding. Label P_1 (P_2 in dashed lines) indicates packet size 8 kbit (1 kbit), and the results obtained with time-varying (time-invariant) channels are labeled as TV (TI) and represented with triangles (circles).

Finally, Fig. 13 shows that the same number of transmissions are generated by the relays in TV channel conditions as L increases, whereas for TI channels, a sparser the network is less connected, and therefore fewer relays transmit a packet, leading to lower energy consumption than in TV channels.

C. Performance comparison in TV and TI channel conditions

In this section, we compare the performance of flooding and SUN in both TV and TI channel conditions. We can see from Fig. 14 that flooding outperforms SUN in terms of throughput in TV channels, whereas in TI channel conditions the performance of SUN with 4 retransmissions (F_4) and short packets (P_2) is better than that of flooding, as shown in Fig. 15.

The first thing to notice from the comparison of the two figures is that in the TI case, where little diversity is available, the performance of both protocols is generally worse.

When the channel is time varying, flooding outperforms the reactive protocol, especially if little error control is implemented and packets are long, unless the network is very dense and

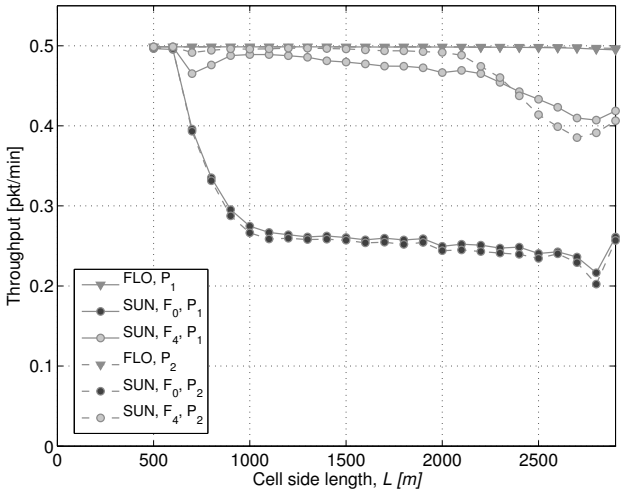

Fig. 14. Throughput as a function of the cell side length L for SUN (circles) and flooding (triangles) for TV channels.

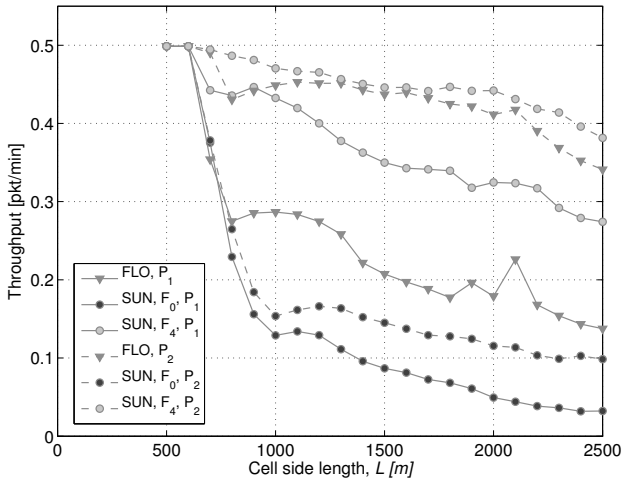

Fig. 15. Throughput as a function of the cell side length L for SUN (circles) and flooding (triangles) for TI channels.

therefore one-hop communication is very reliable. Conversely, the reactive approach with short packets and good reliability (as in F_4) shows a good robustness against prolonged bad link conditions, as its performance shows little degradation when changing from TV to TI, unlike all other schemes.

Even the schemes that achieve the best performance in TV channels, i.e., flooding with both packet sizes, are subject to a very severe performance degradation in the presence of slow channel dynamics (i.e., possibly long outages), especially in the case of long packets, that are the most affected by low SNRs.

In conclusion, we could say that opportunistic and relatively uncoordinated schemes (such as flooding) are a very good option when channel conditions vary in time so as to provide good diversity on the protocol time scales, whereas on the other hand, the only way to operate effectively in a network where outages are prolonged is to provide means to enforce hop-by-hop reliability, e.g., using short packets and/or error control.

D. The impact of constellation size and source level

In this section, we investigate the impact of constellation size and source level. To this aim, we consider an 8PSK modulation scheme and three different source levels: $SL_1 = 145$, $SL_2 = 150$, and $SL_3 = 155$ dB re μPa. In Figs. 16 and 17, we show the throughput obtained by changing

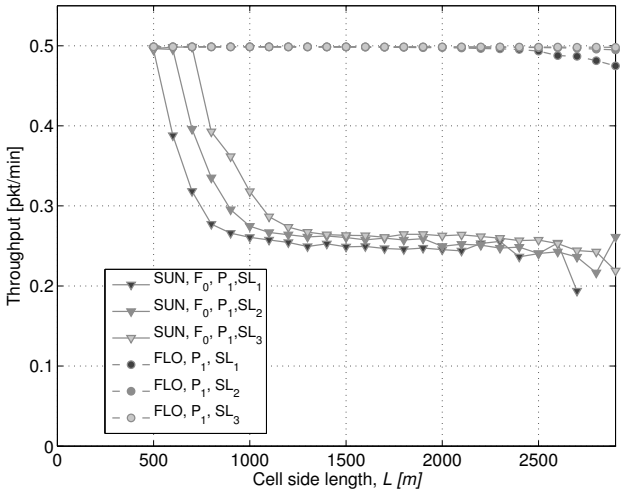

Fig. 16. Throughput as a function of the cell side length L for SUN (triangles) and flooding (circles) for TV channels, packet length P_1, BPSK constellation, and different source levels.

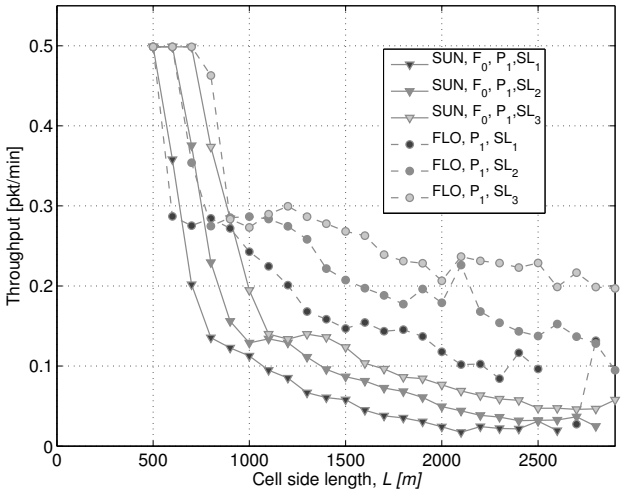

Fig. 17. Throughput as a function of the cell side length L for SUN (triangles) and flooding (circles) for TI channels, packet length P_1, BPSK constellation, and different source levels.

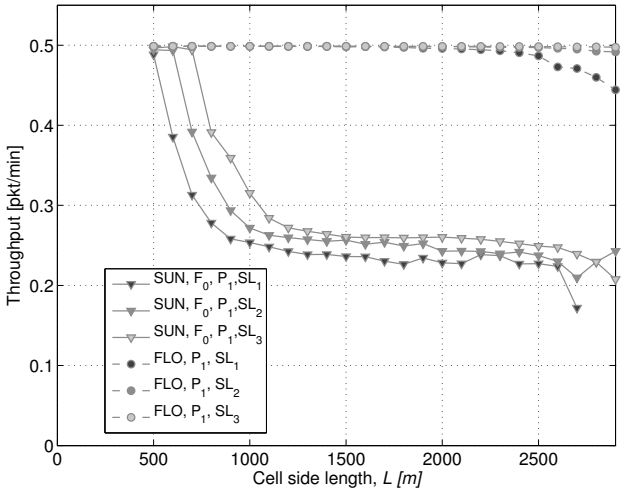

Fig. 18. Throughput as a function of the cell side length L for SUN (triangles) and flooding (circles) for TV channels, packet length P_1, 8PSK constellation, and different source levels.

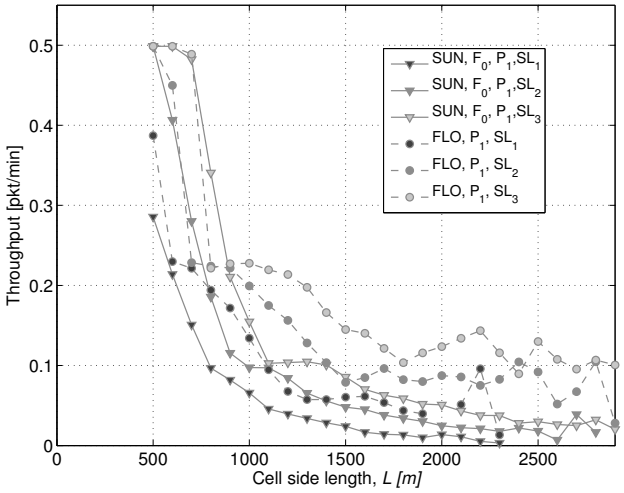

Fig. 19. Throughput as a function of the cell side length L for SUN (triangles) and flooding (circles) for TI channels, packet length P_1, 8PSK constellation, and different source levels.

the source level with a BPSK modulation scheme for both SUN (without retransmissions) and flooding when the longest packet size is chosen in time-varying and time-invariant channel conditions, respectively. We show here only throughput since similar considerations hold for the other metrics.

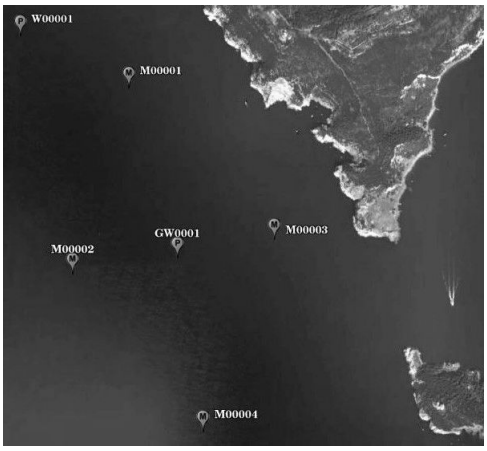

Fig. 20. Scenario of the experiment run during CommsNet12 on October 11, 2012.

Fig. 16 shows that, as the source level increases, the throughput improves and the value of L where multihop starts being used increases, as expected. For example, throughput starts decaying at $L = 900$ m, instead of $L = 700$ m, when source level $SL_3 = 155$ dB re μPa is used instead of $SL_1 = 145$ dB re μPa. The same effect is observed in Fig. 17, where however, with time-invariant channel conditions the performance of flooding is much worse that that obtained with time-varying channels.

Similarly, we consider the case of the 8PSK modulation scheme, with source levels $SL_1 = 145$, $SL_2 = 150$, and $SL_2 = 155$ dB re μPa. Results are shown in Figs. 18 and 19. Larger constellation sizes correspond to increasing the SNR thresholds at which packets start to be unsuccessful, therefore throughput decreases with respect to the case of BPSK, and we observe the same shifting effect towards larger cell sides, as observed in Figs. 16 and 17, when the source level increases.

Therefore, we observed that decreasing (increasing) the constellation size and increasing (decreasing) the source level results in improved (reduced) robustness of the communication system that corresponds to an increased (decreased) threshold distance where multihop paths start being used.

VI. Networking experiments with flooding and SUN during CommsNet12: preliminary results

In this section, we present some preliminary results obtained during the experimental campaign CommsNet12, conducted in collaboration with the NATO Center for Maritime Research and Experimentation (CMRE). The considered experiment took place off the coast of Palmaria Island (Italy), during the morning of October 11, 2012. The deployment scenario is shown in Fig. 20, where each label corresponds to an underwater acoustic device equipped with an S2C 18-34 EvoLogics modem [29]. Such modem uses a semi-coherent modulation scheme, with a center frequency of 25 kHz. The source power level is set to 172 dB re μPa and data packets are around 0.7 s long (therefore similar to case P_2).

The water column is approximately 30 m deep and the bottom can be considered flat in the whole area. Note that in such a shallow water, the sound speed profile is almost constant across the water column, which results into more limited channel quality dynamics. However, the interaction between acoustic signals and time-varying surface conditions causes channel quality fluctuations, albeit different in nature from those based on which we derived our simulation results. As shown in Fig. 20, the network consists of six devices: M4 and W1 are the source and the sink, respectively, and the remaining 4 nodes are relays. The distances among the source and the first row of relays, as well as those from the latter to M1, are approximately 1 km. M1 is around 500 m far from W1. The devices at M1, M2, M3, and M4, are placed on a tripod on the sea bottom, whereas GW1 and W1 have hanging receivers at 25 m and 2 m below the surface, respectively. The traffic model is the same as for simulations. The deployment is chosen such that the sink and source could not communicate with each other, and relays could be thought of as placed in cells of the same side L, as in Fig. 6.

The experimental methodology consists in running one of the routing protocols for an interval of time, that is short enough to consider environmental conditions as stationary and at the same time sufficiently long to collect meaningful statistics for the networking metrics: this interval has been set to 10 minutes. This approach was made possible thanks to the availability and flexibility of the DESERT framework [23].

We first ran flooding for 10 minutes. We observed that the most used link was M4–M1, which then reliably delivered the packets to W1. Packets forwarded by the other relays were received

TABLE I

EXPERIMENTAL RESULTS FOR SUN AND FLOODING DURING COMMSNET12.

	SUN	**flooding**
Throughput [pkt/min]	0.5	1.6
e2e delay [s]	6.9	2.62
average number of hops	2	2.18

subsequently, without interfering with that from M1. Then, we ran SUN for the next 10 minutes. During this phase, the device M1 stopped working, thus leaving only three relays: M2, GW1, and M3. In this scenario, all three links are equally used and the bottleneck is represented by the link to W1.

In order to perform a fair comparison, we post-processed the data so that M1 was not used during flooding. Results in terms of average throughput, end-to-end delivery delay, and number of hops are shown in Table I. The transmission rate was 6 pkt/min. Results confirm those obtained by simulation: flooding outperforms SUN in terms of both throughput and end-to-end delivery delay when data packets are short, only one sink and one source exist in the network, and the topology consists of sufficiently spaced nodes.

VII. CONCLUSIONS

In this paper, we considered the dynamics of the channel conditions over a time scale that is relevant for networking protocols. We computed the performance of two routing protocols by simulation, considering time varying and time invariant channel conditions, as well as different packet lengths and number of retransmissions allowed for each data packet in one of the two protocols. Average throughput, end-to-end delay, and energy consumption metrics were computed and analyzed as a function of different network coverage areas, so as to gain insight on how spatial separation as well as time varying channel conditions play a role in determining and comparing the performance of routing protocols.

Results showed that: i) accounting for and measuring time variability of the acoustic propagation conditions results in a better understanding of the channel quality dynamics observed during experiments at sea; ii) taking into consideration these dynamics provides a more accurate performance evaluation of networking protocols than considering time invariant channel

conditions, as done in the literature so far; iii) protocols with low overhead, such as flooding, outperform a source routing protocol in terms of both throughput and energy consumption in typical underwater acoustic network scenarios, as those considered in this paper. An evaluation of the same metrics studied via simulation is also shown for SUN and flooding in experiments at sea, whose results confirm the insight gained by simulation.

ACKNOWLEDGMENT

This work has been supported by the European Commission under the Seventh Framework Programme (Grant Agreement 258359 – CLAM) and by the Italian Institute of Technology within the Project SEED framework (NAUTILUS project). The authors would like to thank the Woods Hole Oceanographic Institution, Dr. James Preisig and the SPACE08, and KAM11 research personnel for making the data sets available. Many thanks also to the NATO Centre for Maritime Research and Experimentation (CMRE, formerly NURC) for granting us access to the SubNet09 data set and for the collaboration in the CommsNet12 campaign.

REFERENCES

[1] M. Porter, "Bellhop code." [Online]. Available: http://oalib.hlsresearch.com/Rays/index.html

[2] M. Siderius, M. Porter, P. Hursky, V. McDonald, and K. Group, "Effects of ocean thermocline variability on noncoherent underwater acoustic communications," *J. Acoust. Soc. Am.*, vol. 121, no. 4, pp. 1895–1908, 2007.

[3] A. Song, M. Badiey, H. C. Song, W. S. Hodgkiss, M. B. Porter, and the KauaiEx Group, "Impact of ocean variability on coherent underwater acoustic communications during the Kauai experiment (KauaiEx)," *J. Acoust. Soc. Am.*, vol. 123, no. 2, pp. 856–865, 2008.

[4] A. Song, M. Badiey, D. Rouseff, H. C. Song, and W. Hodgkiss, "Range and depth dependency of coherent underwater acoustic communications in KauaiEx," in *Proc. of IEEE OCEANS 2007 - Europe*, Jun. 2007.

[5] M. Badiey, Y. Mu, J. Simmen, and S. Forsythe, "Signal variability in shallow-water sound channels," *IEEE J. Oceanic Eng.*, vol. 25, no. 4, pp. 492–500, Oct. 2000.

[6] N. M. Carbone and W. S. Hodgkiss, "Effects of tidally driven temperature fluctuations on shallow-water acoustic communications at 18 kHz," *IEEE J. Oceanic Eng.*, vol. 25, no. 1, pp. 84–94, Jan. 2000.

[7] A. Song, M. Badiey, H. C. Song, and W. S. Hodgkiss, "Impact of source depth on coherent underwater acoustic communications," *J. Acoust. Soc. Am.*, vol. 128, no. 2, pp. 555–558, 2010.

[8] P. Xie, J. Cui, and L. Lao, "VBF: Vector-based forwarding protocol for underwater sensor networks," in *Proc. of IFIP Networking*, Waterloo, Ontario, Canada, May 2006, pp. 1216–1221.

[9] N. Nicolaou, A. See, P. Xie, J.-H. Cui, and D. Maggiorini, "Improving the robustness of location-based routing for underwater sensor networks," in *Proc. of IEEE OCEANS 2007 - Europe*, Jun. 2007.

[10] J. M. Jornet, M. Stojanovic, and M. Zorzi, "Focused beam routing protocol for underwater acoustic networks," in *Proc. of WUWNet*, San Francisco, California, USA, Sept. 2008.

[11] U. Lee, J. Kong, M. Gerla, J.-S. Park, and E. Magistretti, "Time-critical underwater sensor diffusion with no proactive exchanges and negligible reactive floods," *Ad Hoc Networks*, vol. 5, no. 6, pp. 943–958, 2007.

[12] D. Shin, D. Hwang, and D. Kim, "DFR: an efficient directional flooding-based routing protocol in underwater sensor networks," *Wireless Communications and Mobile Computing*, vol. 12, no. 17, pp. 1517–1527, 2012.

[13] S. Azad, P. Casari, C. Petrioli, R. Petroccia, and M. Zorzi, "On the impact of the environment on MAC and routing in shallow water scenarios," in *Proc. of IEEE OCEANS*, Santander, Spain, Jun. 2011.

[14] F. Guerra, P. Casari, and M. Zorzi, "World Ocean Simulation System (WOSS): a simulation tool for underwater networks with realistic propagation modeling," in *Proc. of WUWNet 2009*, Berkeley, CA, Nov. 2009.

[15] B. Tomasi, J. Preisig, G. B. Deane, and M. Zorzi, "A study on the wide-sense stationarity of the underwater acoustic channel for non-coherent communication systems," in *Proc. of European Wireless*, Vienna, Austria, Apr. 2011.

[16] B. Tomasi, G. Zappa, K. McCoy, P. Casari, and M. Zorzi, "Experimental study of the space-time properties of acoustic channels for underwater communications," in *Proc. of IEEE/OES Oceans*, Sydney, Australia, May 2010.

[17] W. S. Hodgkiss and J. C. Preisig, "Kauai Acomms MURI 2011 (KAM11) experiment," in *Proc. of European Conference on Underwater Acoustics (ECUA)*, 2012, pp. 993–1000.

[18] B. Tomasi, J. Preisig, and M. Zorzi, "On the spatial correlation in shallow water and its impact on networking protocols," in *Proc. of IEEE OCEANS*, Yeosu, South Korea, Jun. 2012.

[19] ——, "On the predictability of underwater acoustic communications performance: the KAM11 data set as a case study," in *Proc. of ACM WUWNet*, Seattle, Washington, 2011.

[20] L. Berkhovskikh and Y. Lysanov, *Fundamentals of Ocean Acoustics*. Springer, 1982.

[21] F. Jensen, W. Kuperman, M. Porter, and H. Schmidt, *Computational Ocean Acoustics*, 2nd ed. New York: Springer-Verlag, 2000.

[22] X. Hong, K. Xu, and M. Gerla, "Scalable routing protocols for mobile ad hoc networks," *IEEE Network*, vol. 16, no. 4, pp. 11–21, Aug. 2002.

[23] R. Masiero, S. Azad, F. Favaro, M. Petrani, G. Toso, F. Guerra, P. Casari, and M. Zorzi, "DESERT Underwater: an NSMiracle-based framework to DEsign, Simulate, Emulate and Realize Test-beds for Underwater network protocols," in *Proc. of IEEE/OES Oceans*, Yeosu, Korea, 2012.

[24] D. B. Johnson and D. A. Maltz, *Mobile Computing*. Kluwer Academic Publishers, February 1996, ch. Dynamic source routing in ad hoc wireless networks, pp. 153–181.

[25] N. Baldo, M. Miozzo, F. Guerra, M. Rossi, and M. Zorzi, "Miracle: The multi-interface cross-layer extension of ns2," *EURASIP Journal on Wireless Communications and Networking*, vol. 2010, no. 1, pp. 761–792, 2010.

[26] R. Urick, *Principles of Underwater Sound*. New York: McGraw-Hill, 1983.

[27] M. Stojanovic, "On the relationship between capacity and distance in an underwater acoustic communication channel," *ACM Mobile Comput. and Commun. Review*, vol. 11, no. 4, pp. 34–43, Oct. 2007.

[28] Kongsberg modem. [Online]. Available: http://www.km.kongsberg.com/ks/web/nokbg0240.nsf/AllWeb/71615F27DDF1E062C12579260039B6C1?OpenDocument

[29] Evologics S2C modems, http://www.evologics.de.